



Experimental evaluation of simulated moving bed reactor for transesterification reaction synthesis of glycol ether ester

Shan Tie¹ · Balamurali Sreedhar² · Megan Donaldson² · Timothy Frank² · Alfred K. Schultz² · Andreas S. Bommarius¹ · Yoshiaki Kawajiri^{1,3}

Received: 13 September 2018 / Revised: 19 February 2019 / Accepted: 26 February 2019 / Published online: 11 March 2019
© Springer Science+Business Media, LLC, part of Springer Nature 2019

Abstract

This work presents an experimental evaluation of multi-column simulated moving bed reactor (SMBR) technology for transesterification of glycol ether ester for the first time. An industrially relevant solvent, propylene glycol methyl ether acetate (DOWANOL™ PMA) was produced using a laboratory-scale SMBR unit packed with a base catalyst. The catalyst selected in this study, a Type-II anion exchange resin, was found to be resistant to deactivation through our experimental runs. To design the SMBR process, single-column experiments were first carried out to develop a mathematical model and estimate model parameters. Using this model, the optimal SMBR process was found by a multi-objective optimization technique to maximize the productivity while achieving high conversions. The optimal operating conditions found in this manner were implemented in the lab-scale SMB unit, which achieved conversions ranging from 47.3 to 57.7%. Furthermore, using the experimental data obtained from these experimental runs, the prediction of the model was improved via Tikhonov regularization, which was successfully validated in an additional run at an even higher conversion of 74.6%.

Keywords Simulated moving bed reactor · Reactive chromatography · Optimization · Glycol ether ester · Anion exchange resin

Nomenclature

A_{cs}	Cross-sectional area of the chromatographic column
EA	Ethyl acetate
C	Liquid phase concentration (mol/L)
D_{ax}	Axial dispersion coefficient (m ² /min)
H	Henry's constant
K_{eq}	Equilibrium constant
k_f	Forward reaction rate constant (L/mol min)
K_m	Mass transfer coefficient (min ⁻¹)
b	Adsorption equilibrium constant
MW	Molecular weight
L	Column length (m)
N	Number

PM	1-methoxy-2-propanol
PMA	Propylene glycol methyl ether acetate
q	Average solid phase concentration (mol/L)
r	Reaction rate (mol/L min)
$SMBR$	Simulated moving bed reactor
t	Time (min)
u	Interstitial velocity in the column (m/min)
U_L	Lower bound on volumetric flow rate (mL/min)
U_U	Upper bound on volumetric flow rate (mL/min)
X	Conversion
x	Axial coordinate

Greek letters

ϵ	Epsilon constraint method
ϵ_T	Total void fraction
ζ	Objective function for SMBR optimization
ξ	Conversion
θ	Parameter
ν	Stoichiometric coefficient
ρ	Tikhonov regularization weighting factor
φ	Objective function for parameter estimation

Superscripts and subscripts

comp	Component
eq	Equilibrium

✉ Yoshiaki Kawajiri
kawajiri@nagoya-u.jp

¹ School of Chemical and Biomolecular Engineering, Georgia Institute of Technology, Atlanta, GA, USA

² The Dow Chemical Company, Midland, MI, USA

³ Present Address: Department of Materials Process Engineering, Nagoya University, Furo-cho, Chikusa, Nagoya 464-8603, Japan

exp	Experiment
rec	Recycle stream
<i>i</i>	Component (EA, PM, PMA, ethanol)
<i>j</i>	Column number (1, 2, 3, 4)
<i>k</i>	Experiment data point
<i>m</i>	Model parameters
<i>D</i>	Desorbent stream
<i>Ex</i>	Extract stream
<i>F</i>	Feed stream
<i>R</i>	Raffinate stream

1 Introduction

Reactive separations offer a competitive economic and environmental alternative to conventional sequential integration of batch reactor and separator operations. This integrated process reduces capital cost because of the combined operation into one apparatus. The conversion in a reactive separation process can exceed the reaction equilibrium because of the simultaneous reaction and separation, where the reaction products are separated and removed from reactants while the reaction proceeds. Many separation principles can be applied to reactive separations, including membrane, crystallization, and chromatography.

Simulated moving bed reactor (SMBR) builds upon the concept of reactive chromatography. The productivity can be increased due to the continuous operation. The pseudo-counter-current operation improves separation resolution, and the internal recycling of desorbent reduces solvent consumption and waste generation (Seidel-Morgenstern et al. 2008). Furthermore, the conversion can be increased because unconsumed reactant is also recycled.

SMBR consists of multiple reactive chromatography columns packed with a resin that is typically both a catalyst and adsorbent material. SMBR (Fig. 1) is operated as a cyclic process consisting of four zones in the standard configuration. There is at least one reactive chromatographic column per zone connected in a cycle. There are two inlet ports for the feed and desorbent and two outlet ports for the extract and raffinate. The switching of the port positions at a regular interval in the direction of the fluid flow simulates the counter-current motion of the stationary phase.

Some past studies addressed production of esters by SMBR (Kawase et al. 1996; Mazzotti et al. 1997). In particular, this work addresses the production of propylene glycol methyl ether acetate (PMA), which is the second-most used ester and has many industry applications as a strong solvent and thus serves as the base for cleaners, paints, and coatings (The Dow Chemical Company 2017). Previously, we demonstrated PMA can be produced by SMBR from an esterification reaction, catalyzed by a cation exchange resin (AMBERLYST™ 15), between acetic acid and

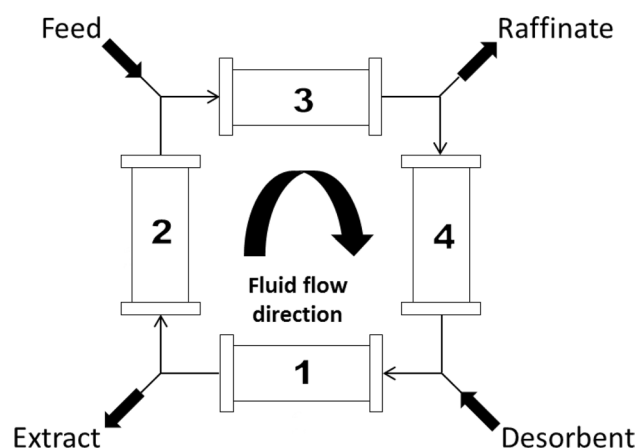


Fig. 1 Schematic of a SMBR operation

1-methoxy-2-propanol to form PMA and the water byproduct (Fig. 2a). We demonstrated development of SMBR utilizing a model based framework (Tie et al. 2016).

In addition to the esterification route discussed above, esters can be produced by transesterification, while reports of this reaction by reactive chromatography or SMBR are scarce. Transesterification in general has many applications demonstrated both in laboratory and industrial scales. In laboratory uses, this organic reaction can be used to prepare esters and polymerization, specifically ring openings of lactones (Martello et al. 2012). In industry, transesterification reactions are performed for paint production through the curing of alkyd resins (Karayannidis et al. 2005). Additionally, transesterification is important for the production of esters of oils and fats (Darnoko and Cheryan 2000). Most recently, with growing interest in environmentally sustainable fuel sources, the potential of biodiesel, fatty acid methyl ester production, which is derived from the transesterification of triglycerides with methanol, has become an attractive option (Fukuda et al. 2001; Meher et al. 2006). However, transesterification is an equilibrium-limited reaction where equilibrium constants are near unity and the reaction rates are low. To overcome the low productivity, the transesterification process has previously been combined with reactive distillation (Noshadi et al. 2012; Pöpken et al. 2001; Steingeweg and Gmehling 2004) and reactive extraction (Shuit et al. 2010; Zakaria and Harvey 2012).

We attempt to explore the transesterification reaction route for PMA production (Fig. 2b) to overcome several disadvantages in the esterification reaction. First, transesterification does not generate water as the byproduct, which forms multiple azeotropes with PM (Hsieh et al. 2006). Consequently, the transesterification route does not require energy intensive downstream operations, such as azeotropic distillation or extractive distillation (Johnson and Wright 1972), for water removal. The absence of water, which adsorbs very

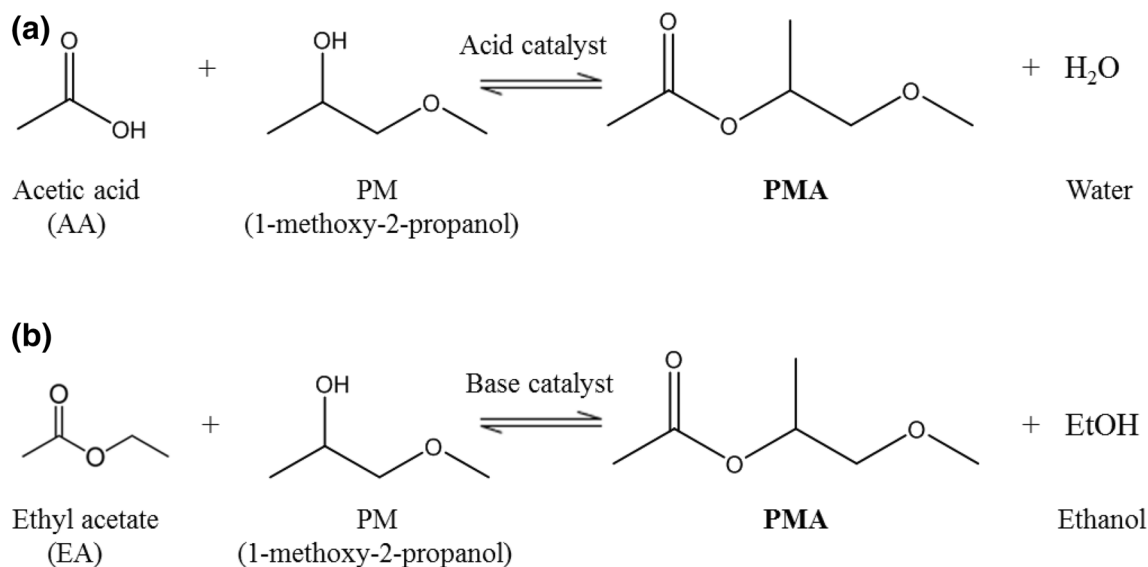


Fig. 2 **a** Esterification reaction, catalyzed by Amberlyst™ 15, between acetic acid and PM to form PMA and water. **b** Transesterification reaction, catalyzed by DOWEX™ 22, between ethyl acetate and PM to form PMA and ethanol

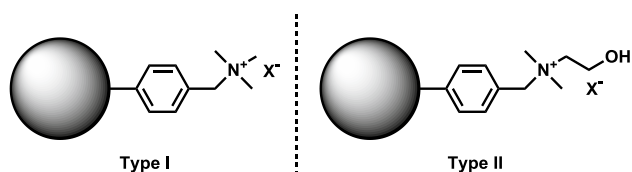


Fig. 3 General structure of type I and II anion exchange resins

strongly to the resin, also reduces desorbent consumption (Oh et al. 2016). Furthermore, transesterification can operate at a much lower temperature, 40–60 °C, compared to that for the esterification, 110 °C, as demonstrated in our previous study (Oh 2015; Oh et al. 2016). We also found that compared to the conventional Type-I resin (Fig. 3a), AMBER-LITE™ IRA904, a Type-II resin (Fig. 3b) DOWEX™ 22 has a substantially longer life of catalytic activity. While we already had these promising findings, experimental tests using an SMBR unit for PMA in the transesterification reaction route has not been conducted yet.

In this work, we apply SMBR to transesterification for the first time for production of PMA. To the best of our knowledge, no previous work has applied reactive chromatography or SMBR technology to transesterification reaction except for biodiesel (Geier and Soper 2010; Johnson and Wright 1972). Moreover, SMBR has yet to be explored for the transesterification production of glycol ether esters (Frank and Donaldson 2016; Oh et al. 2016). We employ the Type-II resin, DOWEX™ 22, which has been found to be resistant against catalytic deactivation. The model and parameters identified from single column chromatography

experiments in (Oh 2016) was employed as the *initial model* parameters, herein referred to as non-SMBR experiments. The *initial model* parameters were refined utilizing SMBR experimental data, and the model is validated.

Furthermore, this paper presents a comparative study of SMBR operation for the transesterification and esterification reaction routes for PMA production. The SMBR operation for the transesterification reaction developed in this work is compared to that of the previous SMBR optimization work for the esterification route (Tie et al. 2016).

2 Methods

This section describes the mathematical model of the SMBR, formulation of the optimization problem, the design and operation of the SMBR unit, and the strategy for correction of the SMBR model.

2.1 Mathematical model of SMBR

The SMBR model along with the initial model parameter values are based on fundamental process equations describing the liquid and solid phase mass balances, adsorption isotherm, and kinetic rate. The initial parameter values are obtained from the previous work (Oh 2016). We consider a pseudo-homogenous reaction mechanism and a transport dispersive model with a linear driving force for the solid phase. The axial dispersion of all components is captured by a lumped dispersion coefficient, D_{ax} , and diffusion into the resin particle by individual components is approximated

by individual mass transfer coefficients, $K_{m,i}$. The transesterification reaction occurs only in the solid phase, which is confirmed from our experimental observation that the reaction does not proceed in the absence of the catalyst.

The main assumptions made in this study are the following: (1) the radial distribution of the liquid concentration can be ignored, (2) the total void fraction ε_T is constant, (3) the adsorptive retention of components and reaction occurs in the solid phase (ion exchange resin), the volume fraction of which is given by $1 - \varepsilon_T$, (4) liquid velocity varies with liquid composition, (5) the linear driving force (LDF) model describes the mass transfer between the liquid and solid phases, (6) the activity coefficient of each component is unity in reaction equilibrium and kinetics, and (7) the transesterification reaction is a reversible, first order reaction with respect to each component. Under these assumptions, the model equations are given as follows.

Mass balance in the liquid phase:

$$\frac{\partial C_i^j(x, t)}{\partial t} + \frac{(1 - \varepsilon_T)}{\varepsilon_T} K_{m,i} (q_i^{j,eq}(x, t) - q_i^j(x, t)) + \frac{1}{\varepsilon_T} \left(u^j(t) \frac{\partial C_i^j(x, t)}{\partial x} + C_i^j(x, t) \frac{\partial u^j(t)}{\partial x} \right) = D_{ax} \frac{\partial^2 C_i^j(x, t)}{\partial x^2} \quad (1)$$

where C_i^j and q_i^j are the concentration in the liquid and the solid phase, respectively, ε_T is the total void fraction, $u^j(t)$ is the superficial velocity of column, D_{ax} is the overall axial dispersion coefficient, $K_{m,i}$ represents the individual mass transfer coefficients, x is the axial distance and t is the time. The superscript j represents the j th column while subscript i refers to the component index. In this work, estimating the void fraction ε_T is difficult, since conventional tracers for ion exchange resins such as polyethylene glycol and blue dextran do not dissolve in PM; it must be estimated together with other parameters as discussed in Sect. 2.4.

Mass balance in the solid phase:

$$\frac{\partial q_i^j(x, t)}{\partial t} = K_{m,i} (q_i^{j,eq}(x, t) - q_i^j(x, t)) + v_i r^j(x, t) \quad (2)$$

where $q_i^{j,eq}$ is the concentration in the solid phase that is in equilibrium with the liquid phase, v_i is the stoichiometric coefficient of the i th component in the esterification reaction and r^j is the net reaction rate in the j th column.

Adsorption equilibrium between the solid and liquid phases is represented by the following equations:

$$q_i^{j,eq}(x, t) = H_i C_i^j(x, t) \quad i = EA, PM, \quad j = 1, \dots, N_{Column}$$

$$q_i^{j,eq}(x, t) = \frac{H_i C_i^j(x, t)}{1 + b_i C_i^j(x, t)} \quad i = PMA, EtOH \quad j = 1, \dots, N_{Column} \quad (3)$$

where H_i is the Henry's constant and b_i is the adsorption equilibrium constant. The symbols EA , PM , PMA , and $EtOH$ refer to ethyl acetate, PM, PMA, and ethanol, respectively and N_{Column} refers to the total number of columns. The decision to use a linear isotherm is for the sake of model simplicity; ethanol and PM can be sufficiently modeled by a linear adsorption isotherm. However, PMA and ethanol demonstrated nonlinear adsorption behavior and is better characterized by a Langmuir isotherm (Oh 2016).

The net reaction rate of the esterification reaction catalyzed by a heterogeneous acid is given by the second order model:

$$r^j = k_1 \left(q_{EA}^j q_{PM}^j - \left(\frac{1}{K_{eq}} \right) q_{PMA}^j q_{EtOH}^j \right) \quad (4)$$

where k_1 is the forward reaction rate constant, K_{eq} is the reaction rate equilibrium constant and r^j is the reaction rate in the j th column.

The above model equations (Eqs. 1–4) describe the concentration profiles in a single-column chromatographic reactor. To extend these equations to describe an SMBR operation, flow and mass balance equations for multiple columns are defined. Flow and mass balance equations are given by:

$$u^{j+1}(t) = u^j(t) - (u_R^j(t) + u_{Ex}^j(t)) + (u_D^{j+1}(t) + u_F^{j+1}(t)) \quad (5)$$

$$C_i^{j+1}(0, t) u^{j+1}(t) = C_i^j(L, t) (u^j(t) - u_{Ex}^j(t) - u_R^j(t)) + C_{i,F} u_F^{j+1}(t) \quad (6)$$

where $u_R^j(t)$, $u_{Ex}^j(t)$, $u_D^j(t)$ and $u_F^j(t)$ are the velocities of raffinate and extract outlet streams, desorbent and feed inlet streams, respectively. These values are positive only if raffinate, extract, desorbent, or feed is withdrawn from or fed to column j , and zero otherwise. The concentration of the i th component in the feed is represented by $C_{i,F}$ and the column length is represented by L .

Finally, a cyclic steady state (CSS) constraint is enforced. At CSS, the concentration profiles at the beginning of the step in the j th column are identical to concentration profiles at the end of the step in the $j + 1$ th column. The formulation is written as:

$$C_i^j(x, 0) = C_i^{j+1}(x, t_{step}), \quad i = EA, PM, PMA, EtOH, \quad j = 1, \dots, N_{Column} - 1 \tag{7}$$

$$q_i^j(x, 0) = q_i^{j+1}(x, t_{step}), \quad i = EA, PM, PMA, EtOH, \quad j = 1, \dots, N_{Column} - 1 \tag{8}$$

$$C_i^{N_{Column}}(x, 0) = C_i^1(x, t_{step}), \quad i = EA, PM, PMA, EtOH \tag{9}$$

$$q_i^{N_{Column}}(x, 0) = q_i^1(x, t_{step}), \quad i = EA, PM, PMA, EtOH \tag{10}$$

where t_{step} is the step time.

The initial SMBR model parameters ($\epsilon_T, K_{eq}, k_1, H_{EA}, H_{PM}, H_{PMA}, H_{EtOH}, D_{ax}, K_{EA}, K_{PM}, K_{PMA}, K_{EtOH}, b_{PMA}, b_{EtOH}$) are determined from three different types of experiments: batch kinetic reaction experiments, unreactive chromatographic pulse tests, and single-column reactive chromatography experiments (Oh 2016). The reaction equilibrium constant K_{eq} and the forward reaction rate k_1 were obtained from a well-stirred batch reactor experiment. All remaining parameters were estimated simultaneously by fitting the model equations for a single-column reactive chromatography model to unreactive pulse tests and single-column reactive chromatography experiments.

2.2 Problem formulation of the optimization problem and solution strategy

The SMBR model presented earlier is integrated into a multi-objective optimization problem. This formulation, a modified version of the one presented by Tie et al. (2016), is summarized below, where six operating parameters—switching time (t_{step}), feed concentration, plus four zone flow rates ($u^j, j = 1, 2, 3, 4$)—are optimized:

Maximize PMA production rate (g/hr):

$$\max \zeta_1 = \frac{A_{cs} MW_{PMA}}{t_{step}} \sum_{j=1}^{N_{Column}} \int_0^{t_{step}} C_{PMA}^j(L, t) u_R^j(t) dt \tag{11}$$

where ζ_1 is the first objective function, A_{cs} is the area of cross-section of the chromatographic column, MW_{PMA} is the molecular weight of PMA, and t_{step} is the switching time. Note that the production rate is defined by the amount of PMA eluting from the raffinate stream only.

Maximize conversion of ethyl acetate:

$$\max \zeta_2 = 1 - \frac{\sum_{j=1}^{N_{Column}} \int_0^{t_{step}} (C_{EA}^j(L, t) u_R^j(t) + C_{EA}^j(L, t) u_{Ex}^j(t)) dt}{\sum_{j=1}^{N_{Column}} \int_0^{t_{step}} C_{EA,F}^j(t) dt} \tag{12}$$

where ζ_2 is the second objective function.

Ethanol content in the raffinate outlet (wt%):

$$\frac{\sum_{j=1}^{N_{Column}} \int_0^{t_{step}} MW_{EtOH} C_{EtOH}^j(L, t) u_R^j(t) dt}{\sum_i \left(\sum_{j=1}^{N_{Column}} \int_0^{t_{step}} MW_i C_i^j(L, t) u_R^j(t) dt \right)} \leq 1\% \tag{13}$$

In this constraint, the ethanol content (Eq. 13) in the raffinate is enforced to be less than 1 wt% for the downstream process.

We also introduce constraints on the zone flow rates to obtain sensible operating conditions and to avoid an excessive pressure drop.

Bounds on the zone flow rates:

$$U_L \leq A_{cs} u^j(t) \leq U_U \tag{14}$$

where U_L and U_U refer to the lower and upper bound, respectively. The upper bound is decided based on the maximum pressure drop that can be experienced by the pumps. In this study, U_L and U_U are set to values corresponding to 0 mL/min and 13.08 mL/min (10 m/hr), respectively. We confirm in Sect. 3.1 that the flow rates in the optimal operations do not reach either of the flow rate bounds.

The optimization of the two objectives is achieved by using an epsilon-constrained method (Kawajiri and Biegler 2006). In this approach, maximization of ζ_2 (Eq. 12) is replaced by the following constraint:

$$\zeta_2 \geq \epsilon \tag{15}$$

By varying the value of ϵ , and repeatedly solving the optimization problem (Eqs. 11–15), a solution set that maximizes PMA production against different conversions is obtained. More details on our approach can be found in a previous study, where trade-offs are analyzed extensively (Agrawal 2014).

The optimization formulations (Eqs. 11–15) form an optimization problem constrained by partial differential equations (PDEs) that is discretized over time and space to form a system of algebraic equations. The spatial domain is discretized into 40 finite elements. The temporal domain is discretized using Radau collocation where one step is discretized into five finite elements and three collocation points. This system of equations forms a nonlinear programming (NLP) problem that is implemented in A Mathematical Programming Language (AMPL) (Fourer 2002). The NLP problem is solved using an interior point solver, IPOPT 3.12 (Wächter 2006).

2.3 SMBR experiments

2.3.1 SMBR column preparation

The four chromatography columns used in the SMBR unit were packed with DOWEX™ 22 resin in the OH⁻ form following the same packing procedure as described previously (Agrawal 2014; Oh 2015). Prior to all SMBR experiments, the resin was regenerated by flowing the columns with 12 bed volumes of 5 wt% NaOH solution, followed by 12 bed volumes of wash in deionized water and then wash in dehydrated PM (dried with molecular sieve).

2.3.2 SMBR unit

The SMBR unit, built in-house, is in a standard four-zone SMB configuration. The entire system (pumps, valves, and detector) is controlled by a MATLAB based graphical user interface developed in house. The SMBR unit is the same unit used in previous work by Tie et al. (2016). The stainless-steel columns are housed in a temperature controlled oven (CH-460 Column Heater, Eppendorf), where the temperature was constantly monitored to ensure the isothermal condition; this is necessary to avoid unexpected influence by the thermal waves caused by the heat of reaction (Sainio et al. 2007). Table 1 lists additional information regarding the experimental conditions for the SMBR system.

$$\phi = \min_{\theta} \sum_{k=1}^{N_{exp}} \sum_{i=1}^{N_{comp}} \left(C_{i,k}^{model} - C_{i,k}^{exp} \right)^2 + \rho \sum_{m=1}^{N_{param}} \left(\frac{\theta_m^{model} - \theta_m^{initial}}{\theta_m^{initial}} \right)^2 \quad (16)$$

$$\theta = (\varepsilon_T, D_{ax}, K_{eq}, k_1, H_{EA}, H_{PM}, H_{PMA}, H_{EtOH}, K_{EA}, K_{PM}, K_{PMA}, K_{EtOH}, b_{PMA}, b_{EtOH})$$

2.3.3 Analysis

Experimental concentrations for each component were determined for the extract and raffinate streams using a Shimadzu gas chromatography (GC) system, GC-2010. The machine

Table 1 Experimental details for the SMBR system

Parameter	Value
Resin	DOWEX™ 22, OH ⁻ form
Number of columns	4
Column length [cm]	50
Column inner diameter [cm]	1.0
Oven temperature [°C]	40

is equipped with a flame ionization detector and a thermal conductivity detector. The column used in the GC analysis is a ZB-1 (Phenomenex) capillary column with dimensions 60 m × 0.32 mm × 1.00 μm. A single method was developed for analysis of all components. A calibration curve was constructed from samples made from known concentrations and the curves were used to determine the concentrations of experimental samples. For more details on the GC method, see (Oh 2015).

2.4 Methodology for model correction

Using the experimental data from the SMBR experiments, the model parameters are corrected to improve the predictability. There are a total of 14 model parameters to be calculated: total void fraction, two reaction kinetic rate constants, four adsorption constants, dispersion coefficient, four mass transfer coefficients, and two equilibrium adsorption constants. The new parameter values are calculated by a least square minimization, which was implemented in AMPL (Fourer 2002).

In this work, an inverse method was used to estimate the new model parameters. The accuracy of the predicted concentration depends on the values of the model parameters. We used a simple least-square technique that minimizes the objective function by correcting the parameter values. The objective function, Φ , is formulated as:

subject to Eqs. 1–10, where C_i refers to the individual component's concentration averaged over a cycle in the raffinate and extract outlets and the averaged concentration over a step in the recycle stream, the subscript k refers to the experiment index, the superscript exp refers to the experimental values, N_{exp} refers to the total number of experiments, and N_{comp} refers to the total number of components. In the second term, N_{param} refers to the total number of parameters in the SMBR model and θ_m refers to the individual parameters. The superscripts $model$ and $initial$ refer to the values given by the SMBR model and those obtained from the initial non-SMBR experiments (Oh 2016). The objective function (Eq. 16) contains two terms; first is the sum of squares of the concentration difference between the model and experimental observations, and the second is known as a Tikhonov regularization (Tikhonov 1995) term that constrains the new parameter estimations from deviating to unrealistic values.

The experimental values C_i^{exp} are obtained from SMBR experiments. After reaching CSS, both raffinate and extract products were sampled over a cycle in a non-disruptive manner. The internal recycle stream at the end of zone IV was sampled only after completing all other sampling since the liquid concentrations is disturbed when the recycle stream is sampled. The same sampling approach was employed by Tie et al. (2016) for parameter correction for the SMBR of the esterification route. All collected samples are analyzed using the method described in Sect. 2.3.3.

Our parameter correction scheme is designed so that parameters are *refined* from the value obtained previously from separate experiments. In Eq. 16, the Tikhonov regularization terms $\rho \sum_{m=1}^{N_{param}} (\theta_m^{model} - \theta_m^{initial} / \theta_m^{initial})^2$ modulate how much the new parameter values differ from the initial values. A large value of ρ weights the Tikhonov terms more heavily in the objective function and thus restricts the new parameter values from large deviations from the original values. Conversely, a small ρ weights the model deviation less strongly and allows for greater deviations in parameter values from the initial values. Good parameter recalculation balances these two terms to allow good model predictions and physically reasonable parameter values. In addition, this regularization is known to reduce the non-uniqueness in ill-posed parameter estimation problems (Tie et al. 2016).

3 Results and discussion

This section describes and discusses results from the optimization of the SMBR system, experiments from the SMBR unit and the details of the parameter estimation for model correction.

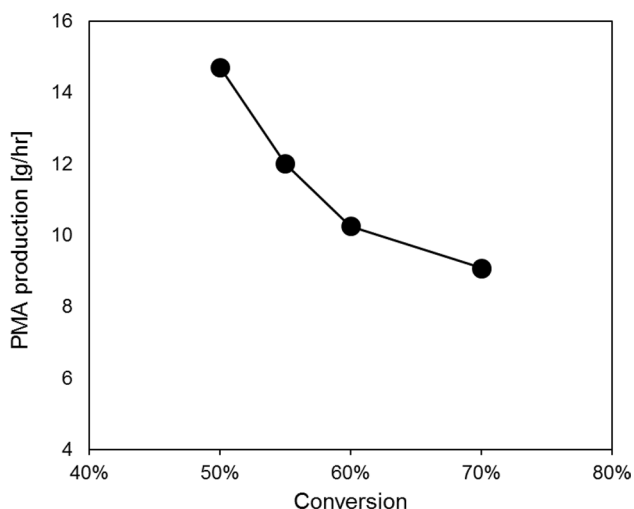


Fig. 4 Pareto plot predicted by model: PMA production rate against conversion of ethyl acetate

3.1 SMBR optimization

The *initial model* is optimized according to the formulations given by Eqs. 11–15. Three different values of ϵ in Eq. 15 are defined, which corresponded to 50%, 60%, and 70% conversion, while solving the maximization problem for ζ_1 (Eq. 11). These conversions are lower than that for the esterification case (Tie et al. 2016), but are within a range of practical interest. The highest conversions we can achieve experimentally were limited by the lower limit of our pump flow rates; if smaller pumps were available that allowed us to operate at lower flow rates, then a higher conversion could be obtained experimentally. Each optimal solution of this optimization problem lies on the Pareto front of the multi-objective optimization problem (Fig. 4). The operating conditions from this multi-objective optimization analysis are shown in Table 2.

Figure 4 shows the Pareto front between PMA production rate (Eq. 11) and conversion (Eq. 12). There is a trade-off relationship between these two objectives. A higher conversion is achieved when the residence time increases inside the SMBR. Consequently, the flow rates decrease and the switch time increases (Table 2). The slower flow rate results in the lower production rate as conversion increases.

Table 2 Optimal operating conditions for SMBR using the *initial model*

	Run 1	Run 2	Run 3
Target conversion [%]	50	60	70
Experimental desorbent flow rate [mL/min]	7.20	6.10	1.30
Experimental extract flow rate [mL/min]	6.10	5.40	0.80
Experimental feed flow rate [mL/min]	0.29	0.18	0.16
Experimental raffinate flow rate [mL/min]	1.40	0.90	0.60
Experimental switch time [min]	6.80	8.30	9.30

Table 3 Experimentally implemented operating conditions for SMBR using the *initial model*

	Run 1	Run 2	Run 3
Conversion predicted by initial model [%]	48.9	59.4	67.4
Desorbent flow rate [mL/min]	7.30	6.10	1.30
Extract flow rate [mL/min]	6.20	5.40	0.80
Feed flow rate [mL/min]	0.30	0.19	0.16
Raffinate flow rate [mL/min]	1.40	0.90	0.70
Switch time [min]	6.80	8.30	9.30

The flow rates reflect the setpoint correction and were rounded off to the nearest 0.1 mL/min when implemented experimentally

3.2 SMBR experiments

The SMBR operating conditions listed in Table 2 are implemented experimentally on the SMBR unit. The operating conditions implemented in experiments and the corresponding conversions predicted by the model are listed in Table 3. The reason there is a difference in the operating conditions and conversions between Tables 2 and 3 is due to the deviations of the actual flow rates from the set points of the pump. The flow rates of the extract and raffinate were measured during the experiments, which are shown in Table 3. On the other hand, for the desorbent and feed flow rates, no direct measurements were possible. For these two pumps, we carried out pump calibration tests, in which the flow rates were indirectly calculated by the change in mass of the feed and desorbent bottles. These tests revealed that the desorbent pump exhibited an error of 2–3% from setpoint. The feed pump had even more deviation from setpoint, 3–8%, because the flow rates were near the lower limit of pump operation. For feed and desorbent flow rates, these flow rate corrections using the calibration curves are reflected in Table 3. The flow rates implemented in the experiments are employed for all model simulation results and the model correction in Sect. 3.3.

Extract and raffinate streams are collected over a cycle in a non-disruptive manner after the SMBR operation reached CSS. The development of CSS was monitored via the refractive index detector on the raffinate line and from sampling the outlets for two consecutive cycles (7 and 8) and observing no change in the conversion. The flow rates for the extract and raffinate streams were measured volumetrically in cylindrical beakers. We observed that it takes nearly six cycles to reach CSS. The concentration of all components is plotted in Fig. 5.

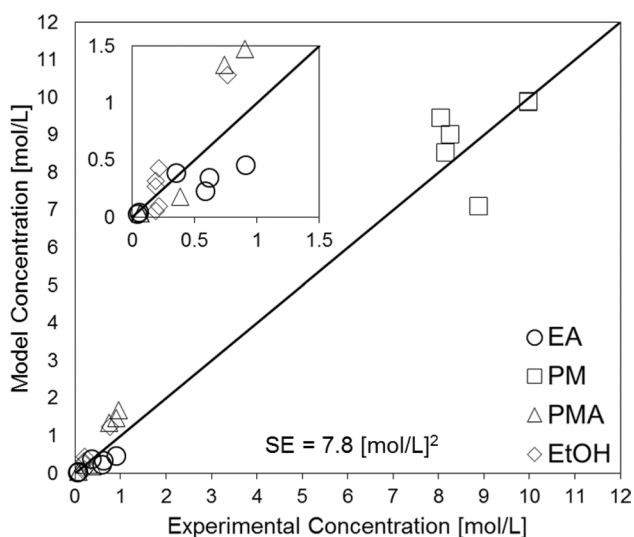


Fig. 5 Comparison of the experiment to the *initial model* prediction for concentrations of all components in the extract and raffinate

The comparison of experimental and model concentrations suggests that the trend of the concentrations is captured well by the model. To quantify the model accuracy, we define the squared error of the concentration:

$$SE = \sum_{k=1}^{N_{\text{exp}}} \sum_{i=1}^{N_{\text{comp}}} (C_{i,k}^{\text{model}} - C_{i,k}^{\text{exp}})^2 \quad (17)$$

These observations demonstrate that the inverse method used on the batch reaction experiments and single-column tests (Oh 2016) to determine model parameters is a reliable method for developing a preliminary SMBR model. The remaining mismatch motivates parameter correction as discussed below.

From our sample collection, we can calculate other performance indicators such as productivity, PMA production rate, conversion, product recovery, byproduct content in the raffinate stream. Table 4 is a summary of the experimental performance indicators for all three conversion experiments. There is significant deviation in the conversion for Run 3 between model prediction and experimental result: 67.4% and 57.7%, respectively. This difference may be due to the model extrapolation; the model parameters were obtained only from single-column experiments, where the highest conversion achieved was only 63% (Oh 2016). The extent of the prior experiments may have limited the accuracy of the model for higher conversions.

3.3 Parameter estimation for model correction

To improve the model accuracy and recalculate model parameters, parameter estimation was carried out using the SMBR experiments. As discussed in Sect. 2.4, there are 14 model parameters, which are refined from the obtained experimental data. Each of the three conversion experiments ($N_{\text{exp}} = 3$) generates samples for all four components ($N_{\text{comp}} = 4$) from the extract and raffinate; hence, there are a total of 24 concentration data points. An appropriate Tikhonov weighting parameter, ρ , from the objective function

Table 4 Summary of experimental performance indicators for all three conversions

	Run 1	Run 2	Run 3
Conversion predicted by initial model [%]	48.9	59.4	67.4
Experimental conversion [%]	47.3	61.7	57.7
Experimental productivity [kg/L/day]	1.26	1.08	0.78
Experimental PMA production rate [g/hr]	8.27	6.60	5.16
Experimental PMA recovery in raffinate [%]	72.3	68.7	67.4
Experimental Ethanol content in raffinate [wt%]	1.09	0.95	1.99

Table 5 Summary of SMBR parameter calculations

Parameter	Total void fraction	Reaction	Adsorption (Henry's constant)				Adsorption (Equilibrium constant)		Dispersion and mass transfer					
			K_{eq}	$k_f [\frac{L}{mol \cdot min}]$	H_{EA}	H_{PM}	H_{PMA}	H_{EtOH}	b_{PMA}	b_{EtOH}	$D_{ax} [\frac{m^2}{min}]$	$K_{EA} [\frac{1}{min}]$	$K_{PM} [\frac{1}{min}]$	$K_{PMA} [\frac{1}{min}]$
<i>Initial model</i>	0.50	0.17	0.105	0.396	0.457	0.206	1.33	0.77	0.296	1.17×10^{-4}	1.12	0.881	1.28	0.80
<i>Corrected model</i>	0.516	0.166	0.096	0.351	0.322	0.238	1.01	0.71	0.303	1.19×10^{-4}	0.304	0.846	1.16	0.19

(Eq. 16) was determined by trial and error such that the optimal solution balances appropriately between model fitting and parameter deviations from the initial values (Hansen and O’Leary 1993). After some trial-and-error runs, the value of ρ was chosen to be 0.1. Table 5 summarizes the SMBR-parameter values from the *initial model* and the *corrected model*. The changes of recalculated parameter values are reasonable compared to the initial values.

The Henry’s constant for PM and ethanol (H_{PM}, H_{EtOH}) changed to improve model fitting. These changes may be accounted for by some key differences in experimental conditions used to obtain the initial to corrected parameter values. First, there is more dead volume in the SMBR experiments that can be lumped into the Henry’s constants (Bentley et al. 2013) calculated for the *corrected model*. Contributing to the dead volumes include the column connection tubing, valves, and pumps. Second, due to the larger number of columns and experiments conducted for the SMBR experiments compared to only the single-column experiments, the variance (error and noise) may not have as great of an impact on the calculations for the *corrected model* values compared to the *initial model* values.

The mass transfer constants for ethyl acetate and ethanol (K_{EA}, K_{EtOH}) changed from their *initial model* values. These changes may be due to strong correlations with the axial dispersion and the Henry’s constants.

A sensitivity analysis was conducted for all the model parameters (Fig. 6). Each parameter was perturbed individually by a 20% increase and decrease from their *corrected model* values while all other parameters were unchanged. The perturbation that yielded the greater change in the squared error is plotted in Fig. 6. There are several sensitive parameters, $\epsilon_T, H_{EA}, H_{PM},$ and H_{PMA} that caused noticeable increases in the squared error (SE) of the concentration (Eq. 17). A few of these parameters are also the same ones that changed by more than 10% from their *initial model* to the *corrected model* values.

There are also some parameters that are not very sensitive. Most of those parameters are the ones whose *corrected model* values remain very close in value to the *initial model* parameter values. One exception is K_{EtOH} ; although it is insensitive from the perturbation study, the parameter value changed greatly from its original *initial model* value to the new *corrected model* value. The reason may be that the parameter value itself changed by over 70% from its original value such that in comparison, the 20% perturbation for the sensitivity analysis is small and the resulting squared error are close to the *corrected model* values.

After parameter recalculation, the *corrected model* simulated the operating conditions from Table 2, the same ones used to conduct the SMBR experiments, to obtain model predictions of the concentrations of all components.

Fig. 6 Summary of the sensitivity analysis. Each parameter was perturbed by 20% while all other parameters were unchanged. The total squared error of the concentration is reported for the *corrected model* along with each perturbed parameter. The asterisk above the bar for ε_T indicates the value extends beyond the maximum y-axis value

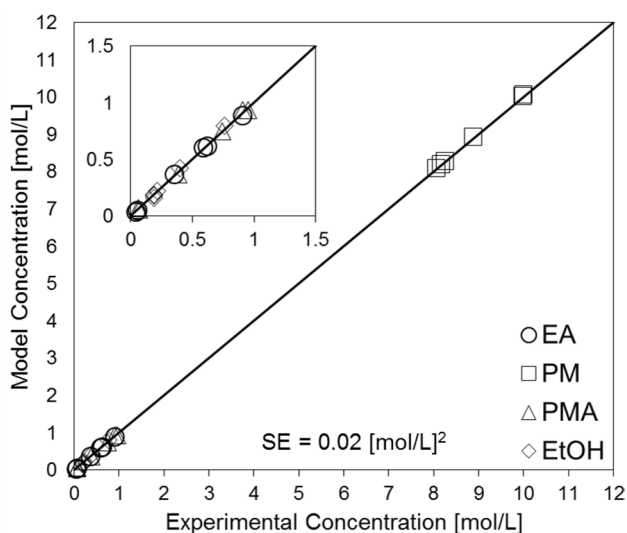
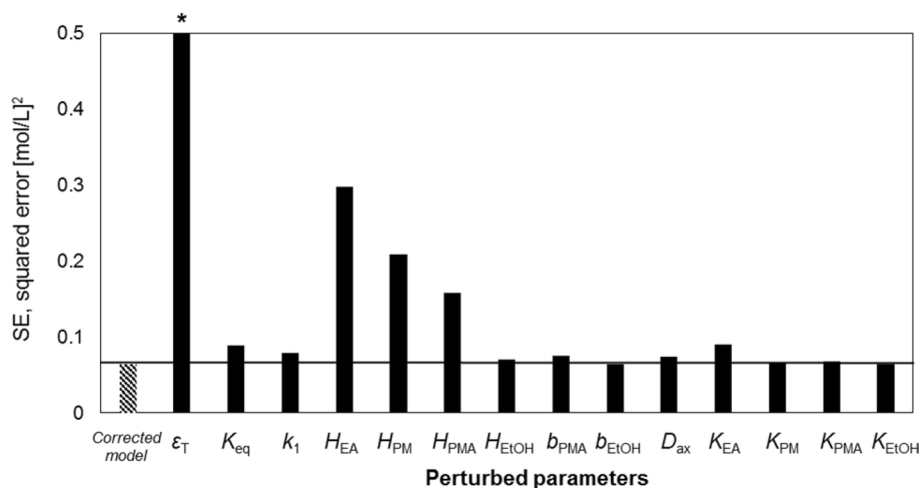


Fig. 7 Comparison of the experiment to the *corrected model* prediction for concentrations of all components in the extract and raffinate

Figure 7 graphs the four component concentrations from the extract and raffinate streams at all three conversion conditions. The plot clearly illustrates the *corrected model* has better fit than the *initial model* and this is quantified by the lower squared error (SE) for the *corrected model*.

3.4 Model validation results

The accuracy of the *corrected model* was verified by a validation experiment. The SMBR operating conditions listed in Table 6 were determined by optimizing the *initial model* to maximize PMA productivity. At these operating conditions, the conversion predicted by the model is 74.8%, which is even higher than the values used in the parameter correction. As can be seen in this table, the experimental conversion 74.6% is very close to the one predicted by the *corrected*

Table 6 Experimental operating conditions and validation result

Operating conditions	
Desorbent [mL/min]	0.41
Extract [mL/min]	0.20
Feed [mL/min]	0.030
Raffinate [mL/min]	0.24
Switch time [min]	29.4
Conversion [%]	
Prediction by initial model [%]	82.6
Prediction by corrected model [%]	74.8
Experiment [%]	74.6

model, which is a significant improvement from the initial model.

Figure 8 compares the experimental observations and model predictions. The *corrected model* (Fig. 8b) shows a greatly improved prediction of the experimental outcomes than the *initial model* (Fig. 8a).

The *corrected model* is also able to describe the production rate (Fig. 9a), conversion (Fig. 9b), and PM–PMA ratio (Fig. 9c) for each experiment significantly more accurately.

3.5 Potential sources of model mismatch

We made several model assumptions (summarized in Sect. 2.1) that may be the source of the remaining model mismatch. First, as discussed in Sect. 3.3, changes in the void fraction due to bed volume changes of the resin can contribute to model error. Second, the reaction may not be second order (Eq. 4) and thus calculations of conversion especially at the higher conversions may change.

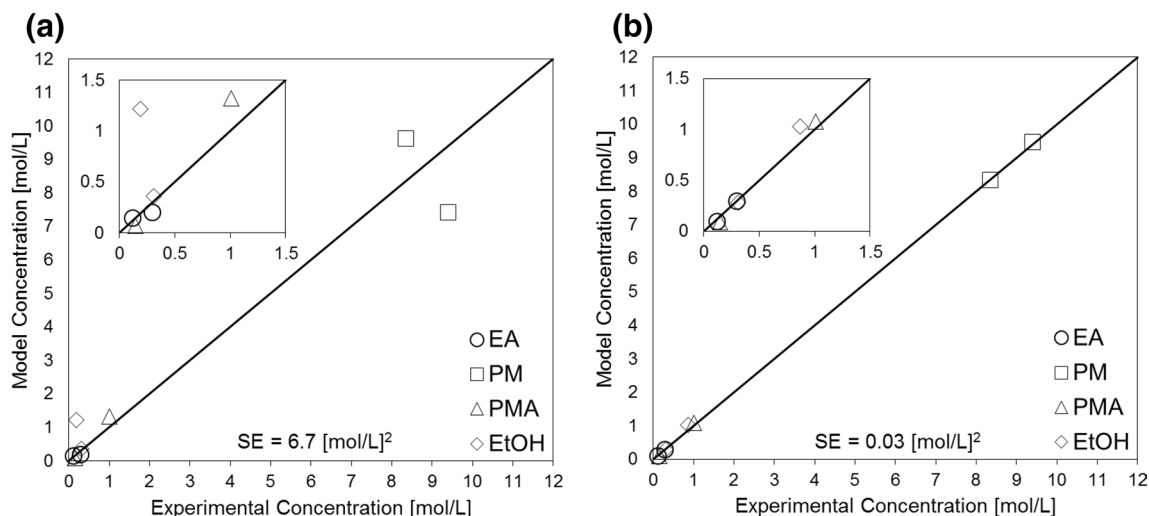


Fig. 8 Comparison of the 80% conversion experiment to the model prediction for **a** initial model and **b** corrected model

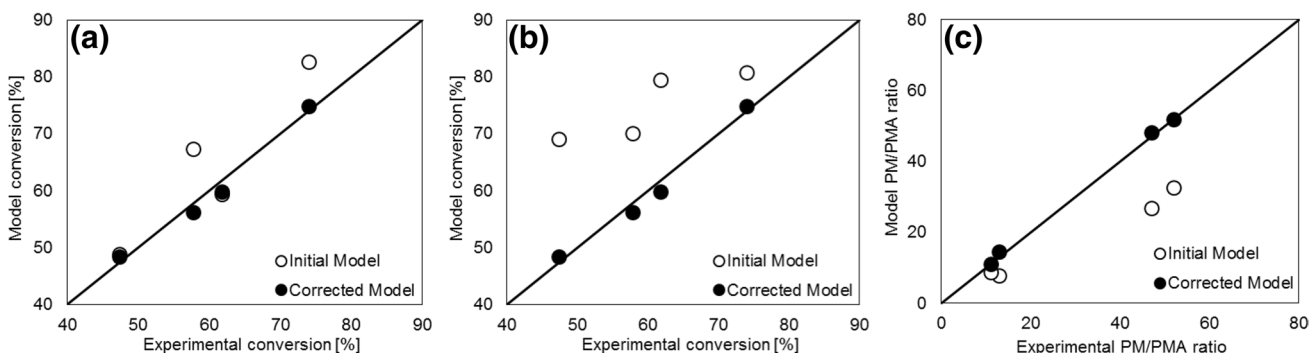


Fig. 9 Comparison plots of **a** production rate, **b** conversion, and **c** PM to PMA ratio

Table 7 Model-based comparison of SMBR production of PMA via the esterification and transesterification routes

Performance indicators	Esterification	Transesterification
Target conversion [%]	90.0	90.0
Production rate [g/hr]	12.2	9.12
Productivity [kg PMA/L/day]	1.87	1.39
N_{PM}/N_{PMA} (mol/mol)	5.00	18.9
Time to cyclic steady state [hr]	19.8	5.66
PMA recovery in the raffinate [%]	99.7	95.3
Byproduct content in raffinate [wt%]	0.49	0.09
Azeotrope	Water	None
Catalyst stability	No deactivation observed	Potential deactivation

3.6 Model-based comparison between esterification and transesterification routes for PMA production

With the *corrected model* developed for both the esterification and transesterification routes, a comparison of their relative performance can be made. Table 7 summarizes the

findings. Esterification features superior productivity/production rate and lower PM–PMA ratio because of the faster reaction rate and higher selectivity of the adsorbent. On the other hand, transesterification has the advantage of shorter time to reach CSS and marginally better recovery and purity in the raffinate outlet.

Each of the two reaction routes has one significant limitation that has not yet been quantified, which are shown in the last two rows in Table 7; for esterification, it is the generation of water and thus the presence of azeotropes. The azeotrope challenge can be overcome by further processing the outlet streams of the SMBR through separation units (Johnson and Wright 1972; Kametaka et al. 1981). Addition of such separation units may offset the higher productivity due to the additional capital and utility cost, which would require further investigation. On the other hand, the transesterification route may have a disadvantage of catalyst deactivation, since base catalysts tend to be more unstable. While we did not observe deactivation in our SMBR experiments in this study, deactivation was observed during accelerated stability studies in which an equal volumetric mixture of ethyl acetate and PM were pumped through a single reactive chromatography column and the PMA and the conversion was measured every hour (Oh 2016). To overcome this potential deactivation, there has been work that demonstrated in situ regeneration of the resin for continuous reactors for biodiesel production (He et al. 2012; Ren et al. 2012; Shibasaki-Kitakawa et al. 2007). In SMBR the regeneration step for the column can be performed by interrupting the production run, which would reduce the productivity. This interruption of production may be avoided by simultaneous regeneration and production by adding the sodium hydroxide solution as a mixture with the solvent through the desorbent inlet (Oh 2016; Oh et al. 2016), or alternatively, offline regeneration of the SMBR columns such that there is periodic regeneration of resin in select columns within a cycle.

It should finally be noted in Table 7 that experimental SMBR conversion for transesterification has not achieved as high of a conversion as 90%. From the reliability of the *corrected model* we observed in the validation experiment, we assumed that the model prediction can be extrapolated to a higher conversion.

4 Conclusion and future work

For production of PMA, we extended our previous work in SMBR optimization and model development to the transesterification reaction pathway. Utilizing the same model-based framework (Tie et al. 2016), the SMBR model is corrected using experimental results from three different conversion experiments. The *corrected model* is validated experimentally at a conversion outside the initial experimental range. This work demonstrates the robustness and applicability of this model-based approach to other applications of SMBR.

The *corrected model* is optimized to target a 90% conversion and the results are compared to those from the esterification route. There are advantages and

disadvantages to either production route for PMA. While the transesterification has lower conversion in our study, developments in resin or the use of alternative catalyst can improve conversion. Another potential route to overcome the limited degrees of freedom in operation of an SMBR is to have different material for the adsorbent and catalyst instead of relying on a single resin to have the ideal properties for both functions (Oh et al. 2016). In this way, a resin adsorbent and a homogenous catalyst can be optimally selected for separation and reaction. Finally, an overall process (Tie et al., in press) that includes downstream separation units and recycle of unreacted reactants for the transesterification route needs to be conducted to allow for a better overall process understanding of this route. Such an investigation will enable a comparative study of the overall process operations between the esterification and transesterification routes.

Acknowledgements We would like to acknowledge the financial support from the University Partnership Initiative at the Dow Chemical Company.

References

- Agrawal, G., Oh, J., Sreedhar, B., Tie, S., Donaldson, M.E., Frank, T.C., Schultz, A.K., Bommarius, A.S., Kawajiri, Y.: Optimization of reactive simulated moving bed systems with modulation of feed concentration for production of glycol ether ester. *J. Chromatogr. A* **1360**, 196–208 (2014)
- Bentley, J., Sloan, C., Kawajiri, Y.: Simultaneous modeling and optimization of nonlinear simulated moving bed chromatography by the prediction–correction method. *J. Chromatogr. A* **1280**, 51–63 (2013)
- Darnoko, D., Cheryan, M.: Kinetics of palm oil transesterification in a batch reactor. *J. Am. Oil Chem. Soc.* **77**, 1263–1267 (2000)
- Fourer, R., Gay, D.M., Kernighan, W.: *MPL. A Modeling Language for Mathematical Programming*. Brooks/Cole Publishing Company, CA (2002)
- Frank, T.C., Donaldson, M.E.: International Patent Application WO2014179706 (2016)
- Fukuda, H., Kondo, A., Noda, H.: Biodiesel fuel production by transesterification of oils. *J. Biosci. Bioeng.* **92**, 405–416 (2001)
- Geier, D., Soper, J.G.: United States Patent US 7828978B2, (2010)
- Hansen, P.C., O’Leary, D.P.: The use of the L-curve in the regularization of discrete ill-posed problems. *SIAM J. Sci. Comput.* **14**, 1487–1503 (1993)
- He, B., Ren, Y., Cheng, Y., Li, J.: Deactivation and in situ regeneration of anion exchange resin in the continuous transesterification for biodiesel production. *Energy Fuels* **26**, 3897–3902 (2012)
- Hsieh, C.-T., Lee, M.-J., Lin, H.: Multiphase equilibria for mixtures containing acetic acid, water, propylene glycol monomethyl ether, and propylene glycol methyl ether acetate. *Ind. Eng. Chem. Res.* **45**, 2123–2130 (2006)
- Johnson, S.H., Wright, H.N.: United States Patent US 3700726A (1972)
- Kametaka, N., Marumo, K., Tokuda, K., Sekiguchi, K.: United States Patent US 4260813A (1981)

- Karayannidis, G.P., Achilias, D.S., Sideridou, I.D., Bikiaris, D.N.: Alkyd resins derived from glycolized waste poly(ethylene terephthalate). *Eur. Polym. J.* **41**, 201–210 (2005)
- Kawajiri, Y., Biegler, L.T.: Nonlinear programming superstructure for optimal dynamic operations of simulated moving bed processes. *Ind. Eng. Chem. Res.* **45**, 8503–8513 (2006)
- Kawase, M., Suzuki, T.B., Inoue, K., Yoshimoto, K., Hashimoto, K.: Increased esterification conversion by application of the simulated moving bed reactor. *Chem. Eng. Sci.* **51**, 2971–2976 (1996)
- Martello, M.T., Burns, A., Hillmyer, M.: Bulk ring-opening transesterification polymerization of the renewable δ -decalactone using an organocatalyst. *ACS Macro Lett* **1**, 131–135 (2012)
- Mazzotti, M., Neri, B., Gelosa, D., Morbidelli, M.: Dynamics of a chromatographic reactor: esterification catalyzed by acidic resins. *Ind. Eng. Chem. Res.* **36**, 3163–3172 (1997)
- Meher, L.C., Sagar, V., Naik, D.: S.N.: Technical aspects of biodiesel production by transesterification—a review. *Renew. Sust. Energ. Rev.* **10**, 248–268 (2006)
- Noshadi, I., Amin, N.A.S., Parnas, R.S.: Continuous production of biodiesel from waste cooking oil in a reactive distillation column catalyzed by solid heteropolyacid: optimization using response surface methodology (RSM). *Fuel* **94**, 156–164 (2012)
- Oh, J.: Development of reactive chromatography system for equilibrium-limited reactions. Ph.D. Thesis, School of Chemical and Biomolecular Engineering, Georgia Institute of Technology, Atlanta, GA, USA (2016)
- Oh, J., Agrawal, G., Sreedhar, B., Donaldson, M.E., Schultz, A.K., Frank, T.C., Bommarius, A.S., Kawajiri, Y.: Conversion improvement for catalytic synthesis of propylene glycol methyl ether acetate by reactive chromatography: experiments and parameter estimation. *Chem. Eng. J.* **259**, 397–409 (2015)
- Oh, J., Sreedhar, B., Donaldson, M.E., Frank, T.C., Schultz, A.K., Bommarius, A.S., Kawajiri, Y.: Transesterification of propylene glycol methyl ether in chromatographic reactors using anion exchange resin as a catalyst. *J. Chromatogr. A* **1466**, 84–95 (2016)
- Pöppen, T., Steinigeweg, S., Gmehling, J.: Synthesis and hydrolysis of methyl acetate by reactive distillation using structured catalytic packings: experiments and simulation. *Ind. Eng. Chem. Res.* **40**, 1566–1574 (2001)
- Ren, Y., He, B., Yan, F., Wang, H., Cheng, Y., Lin, L., Feng, Y., Li, J.: Continuous biodiesel production in a fixed bed reactor packed with anion-exchange resin as heterogeneous catalyst. *Bioresour. Technol.* **113**, 19–22 (2012)
- Sainio, T., Kaspereit, M., Kienle, A., Seidel-Morgenstern, A.: Thermal effects in reactive liquid chromatography. *Chem. Eng. Sci.* **62**, 5674–5681 (2007)
- Seidel-Morgenstern, A., Keßler, L.C., Kaspereit, M.: New Developments in simulated moving bed chromatography. *Chem. Eng. Technol.* **31**, 826–837 (2008)
- Shibasaki-Kitakawa, N., Honda, H., Kuribayashi, H., Toda, T., Fukumura, T., Yonemoto, T.: Biodiesel production using anionic ion-exchange resin as heterogeneous catalyst. *Bioresour. Technol.* **98**, 416–421 (2007)
- Shuit, S.H., Lee, K.T., Kamaruddin, A.H., Yusup, S.: Reactive extraction and in situ esterification of *Jatropha curcas* L. seeds for the production of biodiesel. *Fuel* **89**, 527–530 (2010)
- Steinigeweg, S., Gmehling, J.: Transesterification processes by combination of reactive distillation and pervaporation. *Chem. Eng. Process.* **43**, 447–456 (2004)
- The Dow Chemical Company, Product Safety Assessment: Propylene Glycol Methyl Ether Acetate http://msdssearch.dow.com/PublicLiteratureDOWCOM/dh_096d/0901b8038096dbb5.pdf?filepath=productsafety/pdfs/noreg/233-00407.pdf&fromPage=GetDoc (2017) Accessed June 30 2017
- Tie, S., Sreedhar, B., Agrawal, G., Oh, J., Donaldson, M.E., Frank, T.C., Schultz, A.K., Bommarius, A.S., Kawajiri, Y.: Model-based design and experimental validation of simulated moving bed reactor for production of glycol ether ester. *Chem. Eng. J.* **301**, 188–199 (2016)
- Tie, S., Sreedhar, B., Donaldson, M., Frank, T., Schultz, A., Bommarius, A., Kawajiri, Y.: Process integration for simulated moving bed reactor for production of glycol ether acetate. *Chemical engineering processing—process intensification* (in press)
- Tikhonov, A., Goncharsky, A., Stepanov, V., Yagola, A.: *Numerical Methods for the Solution of Ill-Posed Problems*. Kluwer Academic Publishers, Boston (1995)
- Wächter, A., Biegler, L.T.: On the implementation of an interior-point filter line-search algorithm for large-scale nonlinear programming. *Math. Program.* **106**, 25–57 (2006)
- Zakaria, R., Harvey, A.P.: Direct production of biodiesel from rapeseed by reactive extraction/in situ transesterification. *Fuel Process. Technol.* **102**, 53–60 (2012)

Publisher's Note Springer Nature remains neutral with regard to jurisdictional claims in published maps and institutional affiliations.